Research Square

Preprints are preliminary reports that have not undergone peer review.
They should not be considered conclusive, used to inform clinical practice,
or referenced by the media as validated information.

Reactive Oxygen Species -responsive release of tanshinone IIA for polycystic ovary syndrome treatment

Xiaorong Ni

szy1120@shutcm.edu.cn

Shanghai Municipal Hospital of Traditional Chinese Medicine

Limin Fan

School of Medicine, Tongji University,

Jiani Xie

Shanghai Municipal Hospital of Traditional Chinese Medicine

Jianhua Zhou

Shanghai Municipal Hospital of Traditional Chinese Medicine

Yili Wang

Shanghai Municipal Hospital of Traditional Chinese Medicine

Yijiao Yang

Shanghai Minhang Hospital of Integrated Traditional Chinese and Western Medicine

---

Article

Keywords: MSN@Tan IIA-TK, PCOS, tanshinone IIA, ROS, Inflammation

Posted Date: February 26th, 2026

DOI: https://doi.org/10.21203/rs.3.rs-8721360/v1

License: This work is licensed under a Creative Commons Attribution 4.0 International License.
Read Full License

Additional Declarations: There is **NO** Competing Interest.

Abstract

Polycystic ovary syndrome (PCOS) is a prevalent endocrine disorder often associated with a chronic low-grade inflammatory state, which can elevate oxidative stress and exacerbate PCOS's pathophysiological processes. Natural anti-inflammatory herbal components have been employed for PCOS treatment; however, the challenge lies in effectively targeting these herbal active ingredients due to their poor solubility, low bioavailability, and multiple targets. In this study, we developed a reactive oxygen species (ROS)-sensitive herbal nanomedicine to facilitate the targeted release of active herbal ingredients to PCOS lesions. The herbal nanomedicine, designated MSN@Tan IIA-TK, was formulated by loading the anti-inflammatory herbal compound Tanshinone IIA (Tan IIA) into mesoporous silica nanoparticles (MSN) and grafting a ROS-responsive polymer, mPEG-TK-NHS, onto the surface. Our findings demonstrated that MSN@Tan IIA-TK released Tan IIA in response to elevated ROS levels in PCOS, subsequently reducing oxidative stress and inflammation while promoting the proliferation of ovarian granulosa cells. Further analyses indicated that MSN@Tan IIA-TK effectively mitigated endocrine dysfunction, inflammation, and ovarian damage by inhibiting the ferroptosis pathway. This study highlights the potential of innovative herbal nanomedicines targeting pathological environmental responses in PCOS treatment and offers new perspectives for the clinical application of other traditional herbal therapies.

1. Introduction

Polycystic ovary syndrome (PCOS) is a prevalent endocrine disorder impacting the health of many women of reproductive age globally. It is characterized by cystic ovaries, elevated androgen levels, and menstrual irregularities, often leading to reproductive dysfunction and various metabolic abnormalities. Although the precise cause of PCOS remains unclear, it is believed that genetic, environmental, and lifestyle factors contribute to its development [1]. Current treatments for PCOS encompass medication, surgery, and lifestyle changes. Pharmacological approaches primarily involve the use of oral contraceptives, insulin sensitizers, and anti-androgen medications. These treatments aim to regulate the menstrual cycle, lower androgen levels, induce ovulation, and enhance fertility [1,2]. Surgical interventions primarily consist of ovarian aspiration for egg retrieval, laparoscopic procedures, and the removal of ovarian cysts, all aimed at promoting ovulation and enhancing fertility. Lifestyle modifications, such as dietary changes, weight loss, and regular moderate exercise, are employed to improve insulin resistance, address metabolic disorders, and enhance reproductive health [3]. Nonetheless, these treatments have certain limitations[4]. For instance, discontinuing oral contraceptives after restoring the menstrual cycle can result in the recurrence of menstrual irregularities [5]. Prolonged use of insulin-sensitizing drugs may lead to weight gain and increased insulin resistance. Surgical treatments carry higher risks and have notable recurrence rates, while lifestyle interventions demand long-term commitment and yield variable outcomes. Consequently, the pursuit of novel treatment strategies has become a crucial focus in PCOS research.

Research indicates that PCOS, commonly linked with low-grade systemic inflammation, presents notably elevated levels of circulating inflammatory cells. Additionally, markers of oxidative stress and inflammation correlate positively with androgen levels in individuals with PCOS [6–8]. This inflammatory state likely plays a pivotal role in the pathogenesis and clinical manifestations of PCOS, influencing ovarian function, metabolic regulation, and reproductive health through multiple pathways [6]. Specifically, the inflammatory state can elevate oxidative stress levels, resulting in an imbalance between free radicals and antioxidants in both intracellular and extracellular environments. This imbalance subsequently initiates a cascade of cellular damage and inflammatory responses [9,10]. Therefore, targeting oxidative stress and inflammatory responses may emerge as a crucial strategy in treating PCOS [6].

Numerous components of traditional Chinese herbs are thought to possess anti-inflammatory and endocrine-regulating properties, which could potentially benefit PCOS treatment [11–14]. Herbal medicine is increasingly recognized as a prevalent treatment option for PCOS [12]. Active ingredients from traditional Chinese medicine exert significant therapeutic effects on endocrine regulation, reproductive system function, and clinical symptoms in PCOS patients [15–19]. They represent a valuable adjunct to and support for comprehensive PCOS treatment. Tanshinone IIA (Tan IIA) is a major lipophilic compound extracted from the root of Salvia miltiorrhiza, primarily composed of anthraquinones and terpenoids. Its chemical structure is designated as Phenanthro[1,2-b]furan-10,11-dione, 6,7,8,9-tetrahydro-1,6,6-trimethyl. Highly valued in Traditional Chinese Medicine, Tan IIA has demonstrated therapeutic potential in treating various conditions including cardiovascular disease, inflammation, neurodegenerative diseases, and cancer [20,21]. Research has demonstrated that tanshinone IIA exerts its anti-inflammatory effects by modulating various signaling pathways, including NF-κB, MAPKs, and PI3K/Akt [22–24]. Furthermore, tanshinone IIA has shown significant antioxidant activity, effectively scavenging free radicals, reducing oxidative stress, and shielding cells from oxidative damage [25]. Given these findings, tanshinone IIA has been utilized in the treatment of PCOS. Additionally, it has the potential to regulate hormone levels, restoring balance between estrogen and androgen, and improving insulin sensitivity [26]. This can help reduce insulin resistance levels and alleviate associated symptoms [27]. However, the clinical application of traditional Chinese medicine is hindered by challenges such as low solubility of active ingredients, limited bioavailability, and multiple target sites [28–30]. Therefore, it is crucial to explore methods that can enhance the bioavailability of active ingredients in traditional Chinese medicine and achieve targeted release.

In recent years, the application of nanotechnology in drug delivery has emerged as a promising approach to address these challenges. By encapsulating active ingredients from traditional Chinese medicine into nanocarriers, their solubility, stability, and bioavailability can be enhanced. Moreover, this approach enables targeted release to specific tissues, thereby enhancing therapeutic efficacy while minimizing side effects [31,32]. Here, a ROS-sensitive herbal nanomedicine has been developed for targeted release of herbal active ingredients in the pathological environment associated with PCOS (Scheme 1). This

nanomedicine, composed of mesoporous silica nanoparticles (MSNs) loaded with the anti-inflammatory herbal compound Tan IIA and surface-grafted with the ROS-responsive polymer mPEG-TK-NHS, was designed and synthesized. The study demonstrated that the nanomedicine effectively responds to elevated ROS levels in PCOS by releasing Tan IIA, thereby achieving targeted drug delivery. This approach reduces oxidative stress levels and subsequently suppresses inflammation, promoting proliferation of ovarian granulosa cells. Furthermore, MSN@Tan IIA-TK alleviated endocrine dysfunction, inflammation, and ovarian damage by inhibiting the ferroptosis. The findings highlight the efficacy of MSN@Tan IIA-TK in achieving targeted delivery and therapeutic efficacy of Tan IIA, representing a promising strategy for PCOS treatment at the preclinical level.

2. Results and discussion

TEM results revealed that MSN-Tan IIA exhibited a spherical structure with a rough surface, clearly displaying surface mesopores (Fig. 1A). MSN@Tan IIA-TK was prepared by coating a ROS-responsive cell membrane onto the surface of MSN@Tan IIA, resulting in a discernible thin film structure on its surface, indicating successful modification of the ROS-responsive cell membrane. DLS of the nanoparticles were determined using a Malvern laser particle sizer (Fig. 1B), with MSN@Tan IIA measuring 50.4 ± 1.494 nm and MSN@Tan IIA-TK measuring 160.3 ± 1.494 nm (Fig. 1C). The zeta potential of MSN@Tan IIA-TK (-30.543 ± 0.1443 mV) significantly differed from that of MSN-Tan IIA (-16.51 ± 0.8266 mV), attributed to the ROS-responsive cell membranes loaded with a greater negative potential, confirming successful synthesis of MSN@Tan IIA-TK. Figure 1E illustrates UV absorption peaks of MSN, Tan IIA, and MSN@Tan IIA. MSN exhibited no significant absorption peak between 200–800 nm, while Tan IIA displayed characteristic absorption peaks between 250–280 nm. Upon loading Tan IIA onto MSN, the characteristic peak in MSN@Tan IIA red-shifted and appeared around 284 nm, indicative of successful drug loading, possibly influenced by solvent interactions.

To assess the stability of MSN@Tan IIA and MSN@Tan IIA-TK, changes in nanoparticle hydrodynamic diameters in 5% FBS were monitored using DLS. The results demonstrated that the hydrodynamic diameters of both nanoparticles stabilized around 150 nm and 160 nm within 24 hours, indicating robust structural stability (Fig. 2A). Subsequently, the drug loading efficiency and encapsulation efficiency of Tan IIA were evaluated. As depicted in Fig. 2B and C, MSN@Tan IIA exhibited a drug loading capacity of 25.47 ± 2.06% and an encapsulation efficiency of 68.47%±7.21, while MSN@Tan IIA-TK showed higher values at 28.71%±0.49 and 80.61%±7.21, respectively. These findings confirm efficient loading of Tan IIA onto both MSN@Tan IIA and MSN@Tan IIA-TK. The release profiles of Tan IIA were investigated in PBS solution at pH 7.4, revealing that MSN@Tan IIA and MSN@Tan IIA-TK released approximately 80% and 60% of the drug within 48 hours, respectively (Fig. 2D). The notably slower cumulative release from MSN@Tan IIA-TK suggests that modification with the ROS-responsive cell membrane effectively retards the release rate of Tan IIA, achieving a sustained-release functionality.

To evaluate the ROS scavenging and anti-inflammatory properties of MSN@Tan IIA-TK on Rat Ovarian Granulosa Cells (OGC) in vitro PCOS cell model, high glucose (40 mM) combined with insulin was used

to induce PCOS-like conditions in the cells. The effects of different treatments (PBS, MSN, Tan IIA, MSN@Tan IIA, MSN@Tan IIA-TK) on the cell viability of PCOS cells were investigated initially (Fig. 3A). Compared to the control group, PCOS cell viability was significantly reduced after 24h, 48h, and 72h, and this reduction was significantly reversed after treatment with Tan IIA, MSN@Tan IIA, and MSN@Tan IIA-TK, indicating that Tan IIA effectively mitigated the cellular damage induced by PCOS. Importantly, MSN@Tan IIA-TK exhibited the most pronounced restoration of cell viability. MSN served merely as a carrier without significant impact on cell viability. There was no significant difference between Tan IIA and MSN@Tan IIA in promoting PCOS cell viability (Fig. 3A), highlighting that MSN@Tan IIA-TK, with its modification by the ROS-responsive cell membrane, uniquely inhibited ROS-mediated cell damage and effectively restored cell viability. To confirm the cellular uptake of nanoparticles by PCOS cells, MSN and MSN@Tan IIA-TK were labeled with FITC, resulting in traceable green fluorescence. As shown in Fig. 3B, fluorescence microscopy images demonstrated increasing green fluorescence inside the cells over time, indicating successful nanoparticle endocytosis by PCOS cells. Quantitative flow cytometry assay corroborated these findings, showing enhanced uptake of MSN@Tan IIA-TK by PCOS cells with prolonged incubation (up to 12h) (Fig. 3C).

To verify the inhibitory effect of MSN@Tan IIA-TK on ROS levels within PCOS cells, the ROS probe DCFH-DA was employed. The effect of different treatments (PBS, MSN, Tan IIA, MSN@Tan IIA, MSN@Tan IIA-TK) on intracellular ROS levels in PCOS cells was assessed (Fig. 3D). The fluorescence microscopy images revealed that DCFH-DA green fluorescence, indicative of intracellular ROS levels, was significantly reduced after treatment with Tan IIA, MSN@Tan IIA, and MSN@Tan IIA-TK. Notably, MSN@Tan IIA-TK exhibited the most potent ROS scavenging effect, demonstrating its capability to scavenge ROS and synergistically reduce ROS levels while releasing Tan IIA in response to ROS. Elevated ROS levels often correlate with inflammation, prompting investigation into the anti-inflammatory properties of MSN@Tan IIA-TK on PCOS cells. Levels of inflammation-related factors (IL-6, IL-1β, TNF-α) and activities of superoxide dismutase (SOD), malondialdehyde (MDA), and glutathione peroxidase (GSH-px) were measured (Fig. 3E-K). The results indicated that induction of PCOS significantly increased IL-6, IL-1β, TNF-α, and MDA levels while decreasing SOD and GSH-px activities, indicative of enhanced cellular inflammation. Treatment with Tan IIA, MSN@Tan IIA, and MSN@Tan IIA-TK effectively reduced IL-6, IL-1β, TNF-α, and MDA levels, while enhancing SOD and GSH-px activities, with MSN@Tan IIA-TK demonstrating the most potent anti-inflammatory effects.

In summary, MSN@Tan IIA-TK effectively scavenged elevated ROS levels in PCOS cells and suppressed the expression of inflammation-related factors, highlighting its potential therapeutic efficacy in treating PCOS-associated oxidative stress and inflammation.

Next, we investigated the molecular mechanisms underlying the ROS scavenging and inflammatory suppression effects of MSN@Tan IIA-TK in PCOS cells. PCOS is a multifactorial endocrine disorder with an unclear etiology; however, research suggests it can induce various modes of cell death, including apoptosis, pyroptosis, and ferroptosis [2,33,34]. Therefore, we explored the impact of MSN@Tan IIA-TK on these different cell death pathways in PCOS cells. The flow cytometry assay results indicated a

significant increase in apoptosis levels in PCOS cells compared to the control group, with all Tan IIA treatments showing inhibition of apoptosis, most prominently observed with MSN@Tan IIA-TK treatment (Fig. 4A). The presence of ferroptosis and apoptosis in PCOS cells was confirmed using immunofluorescence and SEM (Fig. 4B and C). MSN@Tan IIA-TK treatment demonstrated superior therapeutic efficacy in both ferroptosis and pyroptosis. Specifically, MSN@Tan IIA-TK treatment increased GPX4 expression levels and decreased ACSL4 expression levels, effectively inhibiting ferroptosis in PCOS cells (Fig. 4B). SEM revealed typical membrane bubbles, ruptured membranes, cell swelling, and evident membrane perforations, characteristic of cellular pyroptosis (Fig. 4C). After MSN@Tan IIA-TK treatment, PCOS cell morphology resembled that of the control group, indicating alleviated pyroptosis.

Ferroptosis is characterized by iron accumulation and lipid peroxidation-driven programmed cell death, associated with excessive ROS production and inflammation-induced reduction of antioxidant capacity. Ferroptosis has been implicated in PCOS pathogenesis [35]. Here, we focused on elucidating the biological mechanism by which MSN@Tan IIA-TK inhibits ferroptosis in PCOS cells. As shown in Fig. 4D and E, qPCR and WB analysis revealed that GPX4 expression was significantly reduced in PCOS cells compared to the control group, while ACSL4, PTGS2, SLC7A11, and CHAC1 expression levels were notably increased. Treatment with Tan IIA, MSN@Tan IIA, and MSN@Tan IIA-TK reversed the expression patterns of these genes and proteins, effectively suppressing cellular ferroptosis. MSN@Tan IIA-TK, with its ROS-responsive drug release capability, demonstrated the most pronounced inhibition of ferroptosis at the molecular level. In conclusion, MSN@Tan IIA-TK effectively reduced ROS levels through Tan IIA release in response to ROS, synergistically lowering ROS levels and effectively inhibiting inflammation. This dual action facilitated the reversal of ferroptosis in PCOS cells.

The therapeutic efficacy of MSN@Tan IIA-TK was investigated in a rat model of PCOS induced by daily subcutaneous injections of dehydroepiandrosterone (DHEA) for 20 consecutive days. To confirm the success of PCOS modeling, estrous cycle changes in rats were assessed. Normal rats have regular estrous cycles of 4–5 days, divided into proestrus, estrus, metestrus, and diestrus stages. Proestrus lasts about 17–21 hours, estrus 9–15 hours, metestrus 10–14 hours, and diestrus 60–70 hours. Proestrus smears show many oval nucleated epithelial cells with occasional cornified cells. Estrus smears show many irregularly shaped cornified epithelial cells with a few nucleated cells. Metestrus smears contain oval nucleated epithelial cells, irregular cornified cells, and leukocytes. Diestrus smears show many leukocytes with a few nucleated epithelial cells. Rats were deemed successfully modeled for PCOS if they lost regular estrous cycles or remained in diestrus. Results indicated that control rats had regular 4–5 day cycles with distinct stages, while modeled rats had disrupted cycles and prolonged diestrus, confirming successful PCOS modeling (Fig. S1). Subsequently, nanomaterials were administered for treatment to assess their therapeutic effects. Serum levels of total testosterone (T), follicle-stimulating hormone (FSH), and luteinizing hormone (LH) were significantly altered in rats with polycystic ovary syndrome (Fig. 5A-C). Using assay kits, serum levels of T, FSH, and LH were measured in various groups of treated PCOS rats. The results demonstrated that Tan IIA treatment reduced serum T and LH levels while significantly increasing FSH levels in PCOS rats, with MSN@Tan IIA-TK showing the

most pronounced therapeutic effect. Changes in inflammatory markers, including IL-6, IL-1β, and TNF-α (Fig. 5D-F), as well as activities of superoxide dismutase (SOD), malondialdehyde (MDA), and glutathione peroxidase (GSH-px) (Fig. 5G-I), were also assessed post-treatment in PCOS rats. Similarly, Tan IIA-containing treatments effectively normalized inflammatory marker levels, with significant alleviation observed in PCOS rats treated with MSN@Tan IIA-TK. Furthermore, changes in fasting glucose (FPG), fasting insulin (FINS), triglycerides (TG), total cholesterol (TC), serum free fatty acids (FFA), estradiol (E2), and progesterone (Prog) levels (Fig. S2) indicated that MSN@Tan IIA-TK had the most significant therapeutic effect in PCOS rats. All Tan IIA-containing groups significantly ameliorated PCOS symptoms, underscoring the therapeutic potential of Tan IIA in PCOS treatment. Importantly, the MSN@Tan IIA-TK group consistently exhibited superior therapeutic efficacy compared to the Tan IIA and MSN@Tan IIA groups, highlighting the pivotal role of nanocarriers in enhancing Tan IIA delivery, intracellular retention, ROS response, and scavenging in the treatment of PCOS.

Next, we investigated the therapeutic effects of MSN@Tan IIA-TK on a rat model of PCOS. Ovarian tissues from rats in each group were stained with HE (Fig. 6A). In the normal group, ovarian tissues exhibited corpus luteum (CL) and cystic follicles (CF) at various stages of development, with neatly arranged granulosa cells. In contrast, ovarian tissues from PCOS rats showed pathological changes characterized by cystic dilation of follicles, multicystic alterations, increased follicle numbers, and loosely arranged granulosa cells. Following MSN@Tan IIA-TK treatment, HE staining results resembled those of normal rats, suggesting restoration of ovarian histopathological changes induced by PCOS.

Furthermore, Tunel staining revealed significantly elevated apoptosis levels in ovarian tissues of PCOS rats compared to the control group. Treatment with Tan IIA, MSN@ Tan IIA, and MSN@Tan IIA-TK inhibited apoptosis, progressively reducing apoptosis levels, with MSN@Tan IIA-TK demonstrating the most significant inhibition (Fig. 6B). Immunofluorescence analysis of ferroptosis-related proteins GPX4 and ACSL4 in ovarian tissues showed that PCOS rats exhibited decreased GPX4 and increased ACSL4 expression compared to the control group (Fig. 6C-D). Treatment with Tan IIA, MSN@Tan IIA, and MSN@Tan IIA-TK restored GPX4 and ACSL4 expression levels, indicating Tan IIA's ability to inhibit cellular ferroptosis and alleviate PCOS symptoms, with MSN@Tan IIA-TK exerting the strongest therapeutic effect, suggesting a synergistic ROS scavenging and Tan IIA treatment effect in PCOS rats. Additionally, qPCR and WB analysis confirmed alleviation of ferroptosis-related gene (ACSL4, PTGS2, SLC7A11, CHAC1, GPX4) expression levels in ovarian tissues of PCOS rats following treatment (Fig. S3). Mitochondrial morphology in ovarian tissues was examined by TEM (Fig. 6E), revealing that PCOS rat mitochondria were swollen, rounded, and had reduced cristae structure compared to normal rat mitochondria. Tan IIA treatment partially restored mitochondrial morphology, with MSN@Tan IIA-TK exhibiting the most pronounced effect, restoring mitochondria to a normal state.

Evaluation of biosafety using HE staining of heart, liver, spleen, lung, and kidney tissues showed no pathological damage in rats from each treatment group (Fig. S4), indicating good biosafety of the treatments. In conclusion, histopathological and molecular assays demonstrated that MSN@Tan IIA-TK

effectively treats PCOS in rats by inhibiting the ferroptosis pathway, while ensuring biosafety, thus highlighting its potential therapeutic efficacy in PCOS treatment.

Polycystic ovary syndrome (PCOS), a prevalent endocrine disorder, affects a substantial number of reproductive-age women worldwide [36–38]. Many components of traditional Chinese herbs are known for their potential anti-inflammatory and endocrine regulatory effects, positioning them as promising candidates for treating PCOS. However, the clinical application of traditional Chinese medicines faces challenges due to the low solubility, limited bioavailability, and the involvement of multiple target sites of their active components [28,29]. In recent years, the application of nanotechnology in drug delivery has introduced innovative approaches to address these challenges. Nanosizing traditional Chinese medicine and encapsulating its active ingredients into nanocarriers have enabled the development of traditional Chinese medicine nanomedicine. This novel therapeutic strategy offers several advantages. Firstly, nanomedicine enhances the solubility and stability of active ingredients from traditional Chinese medicine, thereby improving their bioavailability. Secondly, nanocarriers facilitate targeted delivery to specific tissues, minimizing drug distribution in healthy tissues and thereby reducing side effects. Thirdly, nanomedicines exhibit inherent biological activities that can modulate various biological processes, including inflammatory responses, oxidative stress, and cell signaling [32].

In this study, we developed a ROS-sensitive herbal nanomedicine designed to target PCOS lesions for the controlled release of herbal active ingredients. The nanomedicine, termed MSN@Tan IIA-TK, was formulated by encapsulating the anti-inflammatory herbal component Tan IIA within mesoporous silica nanoparticles (MSN), and then modifying the nanoparticle surface with a ROS-responsive polymer, mPEG-TK-NHS. This innovative approach aimed to enhance the solubility and stability of Tan IIA while enabling its targeted release in response to elevated ROS levels typical of PCOS lesions. By achieving targeted delivery, MSN@Tan IIA-TK increases drug concentration specifically at the site of pathology, thereby significantly enhancing drug bioavailability and efficacy. In our in vitro experiments, MSN@Tan IIA-TK treatment effectively reversed cellular damage induced by PCOS, leading to substantial recovery of cell activity. Mechanistic investigations revealed elevated ROS levels in PCOS model cells, which MSN@Tan IIA-TK efficiently scavenged through the ROS-responsive release of Tan IIA. This synergistic anti-ROS effect of the drug contributed to the restoration of cellular function. Furthermore, MSN@Tan IIA-TK demonstrated potent anti-inflammatory properties by suppressing levels of inflammation-associated factors (IL-6, IL-1β, TNF-α) and modulating activities of superoxide dismutase (SOD), malondialdehyde (MDA), and glutathione peroxidase (GSH-px) in the model cells. These findings underscored the nanomedicine's ability to mitigate oxidative stress and inflammation, thereby restoring cellular function impaired by PCOS-induced pathophysiology. Additionally, our in vivo experiments validated the therapeutic efficacy of MSN@Tan IIA-TK in a PCOS rat model. Treatment with MSN@Tan IIA-TK significantly alleviated serum levels of testosterone (T), follicle stimulating hormone (FSH), luteinizing hormone (LH), inflammatory factors (IL-6, IL-1β, TNF-α), as well as MDA levels, while enhancing GSH and SOD activities. Histopathological and molecular assays further confirmed the safety and effectiveness of MSN@Tan IIA-TK in inhibiting the ferroptosis pathway associated with PCOS.

Importantly, the versatility of the developed targeted-release herbal nanomedicines was highlighted, as the nanocarrier platform can be adapted for delivering various herbal active ingredients. Moreover, by modifying the functional groups responsive to release triggers, such nanocarriers can be tailored to target different disease pathologies with precision.

This study underscores the potential of ROS-sensitive herbal nanomedicine as a promising therapeutic strategy for treating PCOS, offering insights into the development of targeted therapies using traditional herbal medicine in combination with advanced nanotechnology.

3. Materials and methods

Preparation of MSN-Tan IIA

Initially, 1 mL of a 10 mg/mL Tan IIA solution was dissolved in DMSO. Subsequently, 400 μL of the Tan IIA solution was added to 4 mL of a 2 mg/mL MSN solution. The resulting mixture was stirred continuously at 400 rpm for 24 hours. Afterward, the Tan IIA-loaded MSN was subjected to centrifugation and washed several times with water to remove surface-bound Tan IIA. The final product was stored at 4°C.

Preparation of responsive cell membrane

Initially, 1 mg of ovarian granule cell membrane was dispersed in PBS. Then, a specified amount of EDC and NHS was added and allowed to react at room temperature for 6 hours. Following this, 1 mg of mPEG-TK-NH was added and allowed to react for an additional 6 hours. Unreacted reagents were removed by dialysis to obtain ROS-responsive ovarian granule cell membrane.

2Preparation of MSN@Tan IIA-TK

MSN@Tan IIA and ROS-responsive ovarian granule cell membrane were extruded back and forth 20 times using a liposome extruder at a volume ratio of 1:1 to obtain MSN@Tan IIA-TK.

Cell culture

The rat ovarian granulosa cells (OGC) were grown in DMEM/F-12 medium (Gibco, China) with 10% FBS (Gibco) at 37°C in 5% CO2.

Animal

SPF-grade female SD rats, 21 days old and weighing 50 ± 10 g, were supplied by Zhejiang Viton Lever Laboratory Animal Technology Co., Ltd. They were housed at the Experimental Animal Center of Shanghai TCM Hospital under controlled conditions: a temperature of 20°C to 25°C, humidity of 40% to 70%, noise below 60 decibels, 10 to 20 air changes per hour, and a 12-hour light/dark cycle. The rats had

free access to standard and high-fat diets and water. After three days of acclimation in separate cages without any adverse reactions and with normal eating and drinking, they were included in the experiment.

To establish a PCOS model, 21-day-old weaned SPF-grade female SD rats were acclimated for 2 days and then randomly divided into control and model groups. Starting on day 23, the control group received daily subcutaneous injections of 0.4 mL saline in the neck and 0.3 mL saline in the abdomen for 30 days, with free access to standard feed and water. The model group received daily subcutaneous injections of DHEA (6 mg/100 g) in 0.4 mL water for injection in the neck and 0.3 mL HCG solution (1.5 IU/rat) in the abdomen for 30 days, with free access to a high-fat diet and 5% glucose water. Rats were weighed weekly. Starting on day 43, vaginal smears were monitored to preliminarily determine the success of the model based on the estrous cycle. Except for the control group, all other rats received daily intraperitoneal injections of GnRHa (40 μg/100 g). On the ninth day (after successful PCOS induction), they also received PMSG (40 IU/100 g) and HCG (100 IU/100 g) 48 hours later.

Assessment of estrous cycles

Estrous cycles were examined daily between 8:00–9:00 AM. Vaginal lavage fluid with 0.9% saline was thinly spread on microscope slides. After air-drying, slides were stained with 0.1% toluidine blue for 2 seconds at room temperature. Diestrus, estrus, and proestrus stages were identified based on the presence of leukocytes, nucleated cells, and cornified cells.

Statistical analysis

The experimental data were analyzed using GraphPad Prism v.8.4.0 software (GraphPad, USA). The results are shown as the mean ± SD. The differences between any two groups were determined by the T-test. One-way analysis of variance (ANOVA) was used to compare differences among two or more groups. ns represented not significant, ****P < 0.0001, ***P < 0.001, **P < 0.01, *P < 0.05. All data were repeated independently at least three times.

4. Conclusion

Herbal components with natural anti-inflammatory properties have demonstrated efficacy in treating polycystic ovary syndrome (PCOS). However, these herbal active ingredients face inherent challenges in disease treatment, such as low solubility, limited bioavailability, and multitarget effects. To overcome these obstacles, we encapsulated Tan IIA within mesoporous silica nanoparticles (MSN) to enhance its solubility. Subsequently, we surface-functionalized MSN with a ROS-responsive polymer, mPEG-TK-NHS, enabling Tan IIA release in response to elevated ROS levels at PCOS sites. This approach achieved targeted delivery of Tan IIA, enhancing the bioavailability of the drug. This study highlights the significant potential of newly developed herbal nanomedicines that respond to pathological environments in treating PCOS. It also offers insights into the clinical application of targeted therapies using traditional herbal medicine.

Declarations

Ethics approval and consent to participate

Written informed consent was obtained from each participant and the study was approved by the ethical committee of Shanghai Municipal Hospital of Traditional Chinese Medicine, Shanghai University of Traditional Chinese Medicine (ethical approval number: 2023035).

Consent for publication

Not applicable.

Competing interests

The authors declared that no competing interest exists.

Author contributions

Limin Fan: conceptualization, investigation, data curation, formal analysis, visualization, writing—original draft;

Acknowledgements

This study obtained support from a grant from the National Natural Science Foundation of China (Grant No. 81804136), Shanghai Medical Innovation Development Foundation (No. WL-HBMS-2021003K, WLJH2022ZY-ZYY005).

Availability of data and materials

The data are available from the corresponding author upon reasonable request.

References

1. Teede, H. J. *et al.* Recommendations from the international evidence-based guideline for the assessment and management of polycystic ovary syndrome. *Hum Reprod* **33**, 1602–1618, doi:10.1093/humrep/dey256 (2018).
2. Escobar-Morreale, H. F. Polycystic ovary syndrome: definition, aetiology, diagnosis and treatment. *Nat Rev Endocrinol* **14**, 270–284, doi:10.1038/nrendo.2018.24 (2018).
3. Moran, L. J., Pasquali, R., Teede, H. J., Hoeger, K. M. & Norman, R. J. Treatment of obesity in polycystic ovary syndrome: a position statement of the Androgen Excess and Polycystic Ovary Syndrome Society. *Fertil Steril* **92**, 1966–1982, doi:10.1016/j.fertnstert.2008.09.018 (2009).

4. Yang, Y. J. *et al.* Tanshinone for polycystic ovary syndrome A protocol of systematic review and meta-analysis. *Medicine* **100**, doi:ARTN e242810.1097/MD.0000000000024287 (2021).
5. Nestler, J. E. Metformin for the treatment of the polycystic ovary syndrome. *New Engl J Med* **358**, 47–54, doi:DOI 10.1056/NEJMct0707092 (2008).
6. Velez, L. M., Seldin, M. & Motta, A. B. Inflammation and reproductive function in women with polycystic ovary syndrome. *Biol Reprod* **104**, 1205–1217, doi:10.1093/biolre/ioab050 (2021).
7. Ojeda-Ojeda, M., Murri, M., Insenser, M. & Escobar-Morreale, H. F. Mediators of Low-Grade Chronic Inflammation in Polycystic Ovary Syndrome (PCOS). *Curr Pharm Design* **19**, 5775–5791, doi:Doi 10.2174/1381612811319320012 (2013).
8. González, F., Rote, N. S., Minium, J. & Kirwan, J. P. Reactive oxygen species-induced oxidative stress in the development of insulin resistance and hyperandrogenism in polycystic ovary syndrome. *J Clin Endocr Metab* **91**, 336–340, doi:10.1210/jc.2005-1696 (2006).
9. Mittal, M., Siddiqui, M. R., Tran, K., Reddy, S. P. & Malik, A. B. Reactive Oxygen Species in Inflammation and Tissue Injury. *Antioxid Redox Sign* **20**, 1126–1167, doi:10.1089/ars.2012.5149 (2014).
10. Jyoti, A., Mishra, N. & Dhas, Y. Ageing: consequences of excessive free radicals and inflammation. *Curr Sci India* **111**, 1787–1793, doi:10.18520/cs/v111/i11/1787-1793 (2016).
11. Jin, J. *et al.* Tanshinone IIA attenuates estradiol-induced polycystic ovarian syndrome in mice by ameliorating FSHR expression in the ovary. *Exp Ther Med* **17**, 3501–3508, doi:10.3892/etm.2019.7352 (2019).
12. Shen, W. J. *et al.* Effects of tanshinone on hyperandrogenism and the quality of life in women with polycystic ovary syndrome: protocol of a double-blind, placebo-controlled, randomised trial. *Bmj Open* **3**, doi:ARTN e003646 10.1136/bmjopen-2013-003646 (2013).
13. Mohammed, S., Cockburn, B. N. & Sundaram, V. Exploring the Novel Alternative and Modern Treatment Options for Polycystic Ovary Syndrome-A Review. *Integr Med Rep* **3**, 33–42, doi:10.1089/imr.2023.0045 (2024).
14. Raja-Khan, N., Stener-Victorin, E., Wu, X. & Legro, R. S. The physiological basis of complementary and alternative medicines for polycystic ovary syndrome (vol 301, pg E1, 2011). *Am J Physiol-Endoc M* **303**, E1506–E1506, doi:10.1152/ajpendo.zh1-6726-corr.2011 (2012).
15. Zhou, X. *et al.* Efficacy and safety of Chinese patent medicine Xiao Yao San in polycystic ovary syndrome: A systematic review and meta-analysis. *J Ethnopharmacol* **313**, doi:ARTN 11651710.1016/j.jep.2023.116517 (2023).
16. Choi, J. H. *et al.* Korean Red Ginseng alleviates dehydroepiandrosterone-induced polycystic ovarian syndrome in rats via its antiinflammatory and antioxidant activities. *J Ginseng Res* **44**, 790–798, doi:10.1016/j.jgr.2019.08.007 (2020).
17. Jazani, A. M., Azgomi, H. N. D., Azgomi, A. N. D. & Azgomi, R. N. D. A comprehensive review of clinical studies with herbal medicine on polycystic ovary syndrome (PCOS). *Daru* **27**, 863–877, doi:10.1007/s40199-019-00312-0 (2019).

18. Chen, H. Z., Deng, C. J., Meng, Z. Y. & Meng, S. X. Effects of TCM on polycystic ovary syndrome and its cellular endocrine mechanism. *Front Endocrinol* **14**, doi:ARTN 95677210.3389/fendo.2023.956772 (2023).
19. Fu, L. W. *et al.* Traditional Chinese medicine formulae: A complementary method for the treatment of polycystic ovary syndrome. *J Ethnopharmacol* **323**, doi:ARTN 117698 10.1016/j.jep.2023.117698 (2024).
20. Wang, X. H., Morris-Natschke, S. L. & Lee, K. H. New developments in the chemistry and biology of the bioactive constituents of Tanshen. *Med Res Rev* **27**, 133–148, doi:10.1002/med.20077 (2007).
21. Ansari, M. A. *et al.* Prospective therapeutic potential of Tanshinone IIA: An updated overview. *Pharmacol Res* **164**, doi:ARTN 10536410.1016/j.phrs.2020.105364 (2021).
22. Zhang, R., Liu, Y. E., You, J. H. & Ge, B. P. Tanshinone IIA inhibits ischemia-reperfusion-induced inflammation, ferroptosis and apoptosis through activation of the PI3K/Akt/mTOR pathway. *Hum Exp Toxicol* **42**, doi:Artn 09603271231180864 10.1177/09603271231180864 (2023).
23. Ding, B. *et al.* Tanshinone IIA attenuates neuroinflammation via inhibiting RAGE/NF-κB signaling pathway in vivo and in vitro. *J Neuroinflamm* **17**, doi:ARTN 30210.1186/s12974-020-01981-4 (2020).
24. Jin, H., Peng, X. Q., He, Y. Y., Ruganzu, J. B. & Yang, W. N. Tanshinone IIA suppresses lipopolysaccharide-induced neuroinflammatory responses through NF-κB/MAPKs signaling pathways in human U87 astrocytoma cells. *Brain Res Bull* **164**, 136–145, doi:10.1016/j.brainresbull.2020.08.019 (2020).
25. Quan, M. X. *et al.* Tanshinone IIA protects against lipopolysaccharide-induced lung injury through targeting Sirt1. *J Pharm Pharmacol* **71**, 1142–1151, doi:10.1111/jphp.13087 (2019).
26. Bai, L. *et al.* Tanshinone IIA enhances the ovarian reserve and attenuates ovarian oxidative stress in aged mice. *Vet Med Sci* **8**, 1617–1625, doi:10.1002/vms3.811 (2022).
27. Hwang, S. L. *et al.* Tanshinone IIA improves endoplasmic reticulum stress-induced insulin resistance through AMP-activated protein kinase. *Biochem Bioph Res Co* **430**, 1246–1252, doi:10.1016/j.bbrc.2012.12.066 (2013).
28. Shang, Q. *et al.* Nano-formulated delivery of active ingredients from traditional Chinese herbal medicines for cancer immunotherapy. *Acta Pharm Sin B* **14**, 1525–1541, doi:10.1016/j.apsb.2023.12.008 (2024).
29. Kang, C. L. *et al.* Smart Targeted Delivery Systems for Enhancing Antitumor Therapy of Active Ingredients in Traditional Chinese Medicine. *Molecules* **28**, doi:ARTN 595510.3390/molecules28165955 (2023).
30. Rao, S. Y. *et al.* Traditional Chinese medicine active ingredients-based selenium nanoparticles regulate antioxidant selenoproteins for spinal cord injury treatment. *J Nanobiotechnol* **20**, doi:ARTN 27810.1186/s12951-022-01490-x (2022).
31. Shi, J. J., Kantoff, P. W., Wooster, R. & Farokhzad, O. C. Cancer nanomedicine: progress, challenges and opportunities. *Nat Rev Cancer* **17**, 20–37, doi:10.1038/nrc.2016.108 (2017).

32. Zheng, Y. H. *et al.* The combination of nanotechnology and traditional Chinese medicine (TCM) inspires the modernization of TCM: review on nanotechnology in TCM-based drug delivery systems. *Drug Deliv Transl Re* **12**, 1306–1325, doi:10.1007/s13346-021-01029-x (2022).
33. Li, D. *et al.* Autophagy is activated in the ovarian tissue of polycystic ovary syndrome. *Reproduction* **155**, 85–92, doi:10.1530/Rep-17-0499 (2018).
34. Liu, H. L. *et al.* Cryptotanshinone Protects against PCOS-Induced Damage of Ovarian Tissue via Regulating Oxidative Stress, Mitochondrial Membrane Potential, Inflammation, and Apoptosis via Regulating Ferroptosis (Retracted Article). *Oxid Med Cell Longev* **2022**, doi:Artn 801185010.1155/2022/8011850 (2022).
35. Wang, F. X. *et al.* BNC1 deficiency-triggered ferroptosis through the NF2-YAP pathway induces primary ovarian insufficiency. *Nat Commun* **13**, doi:ARTN 587110.1038/s41467-022-33323-8 (2022).
36. Teede, H. J. *et al.* Recommendations from the 2023 International Evidence-based Guideline for the Assessment and Management of Polycystic Ovary Syndrome. *Fertil Steril* **120**, 767–793, doi:10.1016/j.fertnstert.2023.07.025 (2023).
37. Agarwal, A., Aponte-Mellado, A., Premkumar, B. J., Shaman, A. & Gupta, S. The effects of oxidative stress on female reproduction: a review. *Reprod Biol Endocrin* **10**, doi:Artn 4910.1186/1477-7827-10-49 (2012).
38. Yan, S. S. *et al.* Nanocomposites based on nanoceria regulate the immune microenvironment for the treatment of polycystic ovary syndrome. *J Nanobiotechnol* **21**, doi:ARTN 41210.1186/s12951-023-02182-w (2023).

Scheme 1

Scheme 1 is available in the Supplementary Files section.

Figures

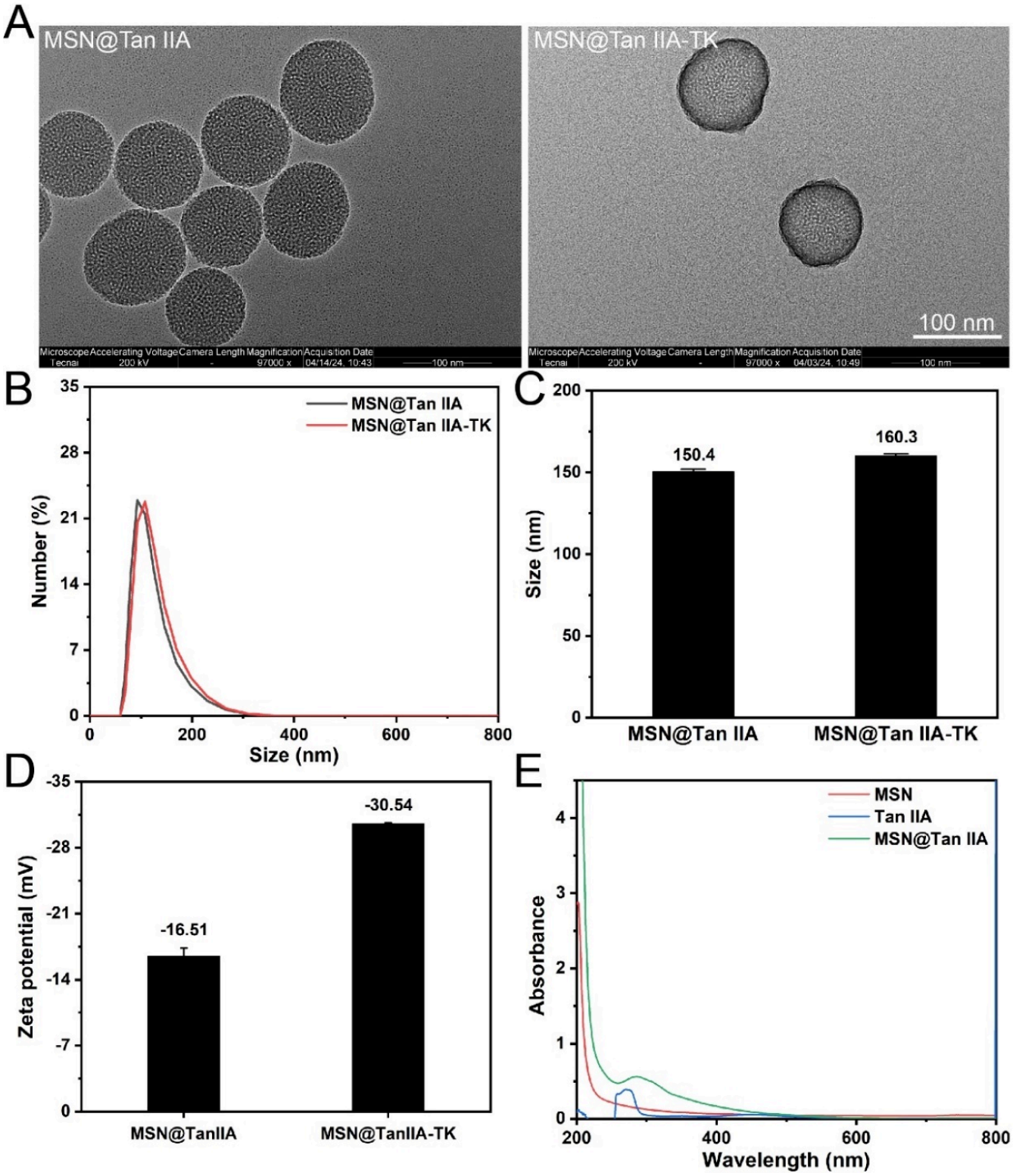


Figure 1

Characterization of MSN@Tan IIA and MSN@Tan IIA-TK. (A) TEM images, (B) DLS, (C) particle size statistics, (D) zeta potential and (E) UV absorption spectra.

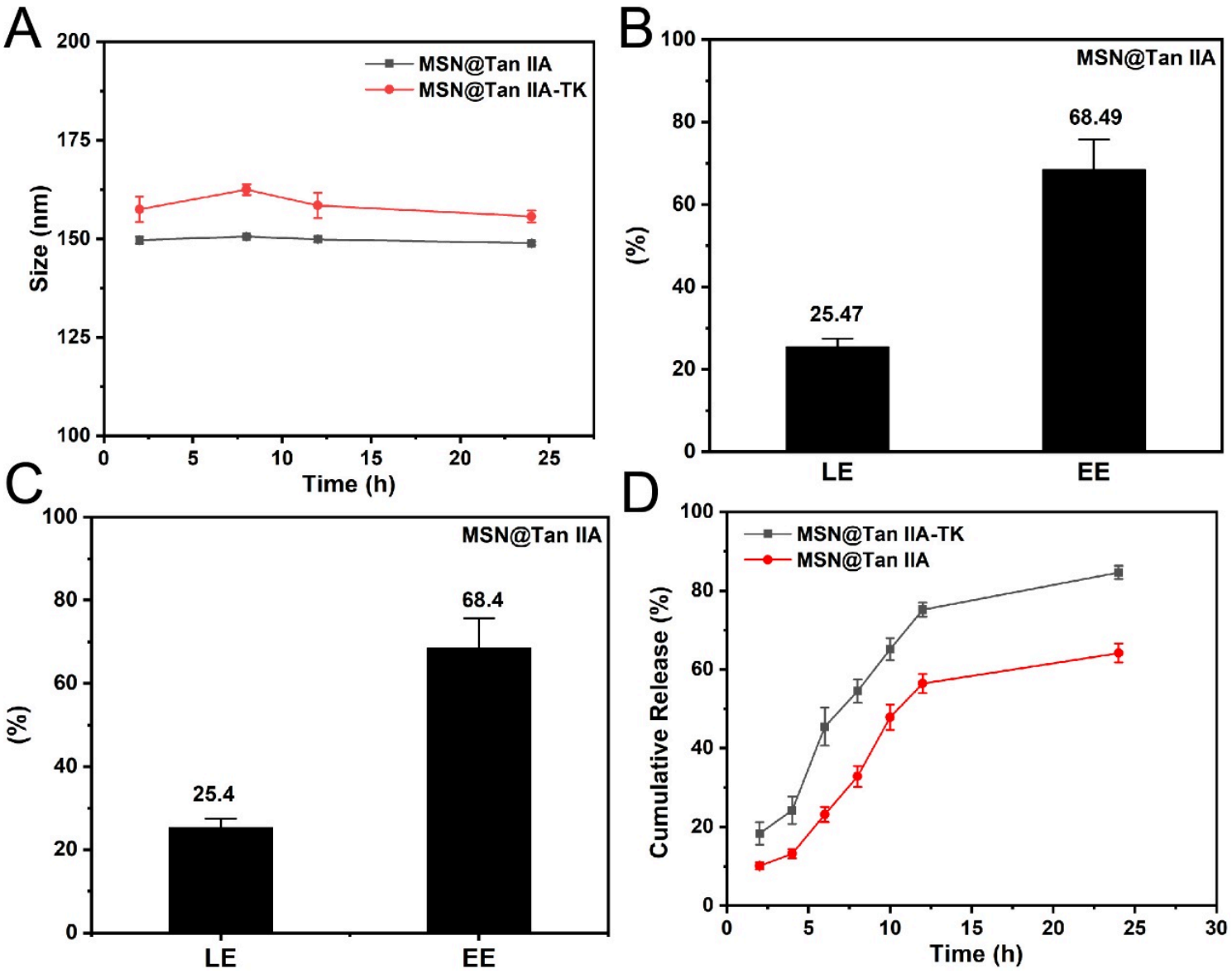


Figure 2

Characterization of stability and release properties of MSN@Tan IIA and MSN@Tan IIA-TK. (A) DLS was used to characterize particle size stability; (B) and (C) UV spectrophotometer detection of loading (LE) and encapsulation (EE) of different nanoparticles of Tan IIA; and (D) release of Tan IIA.

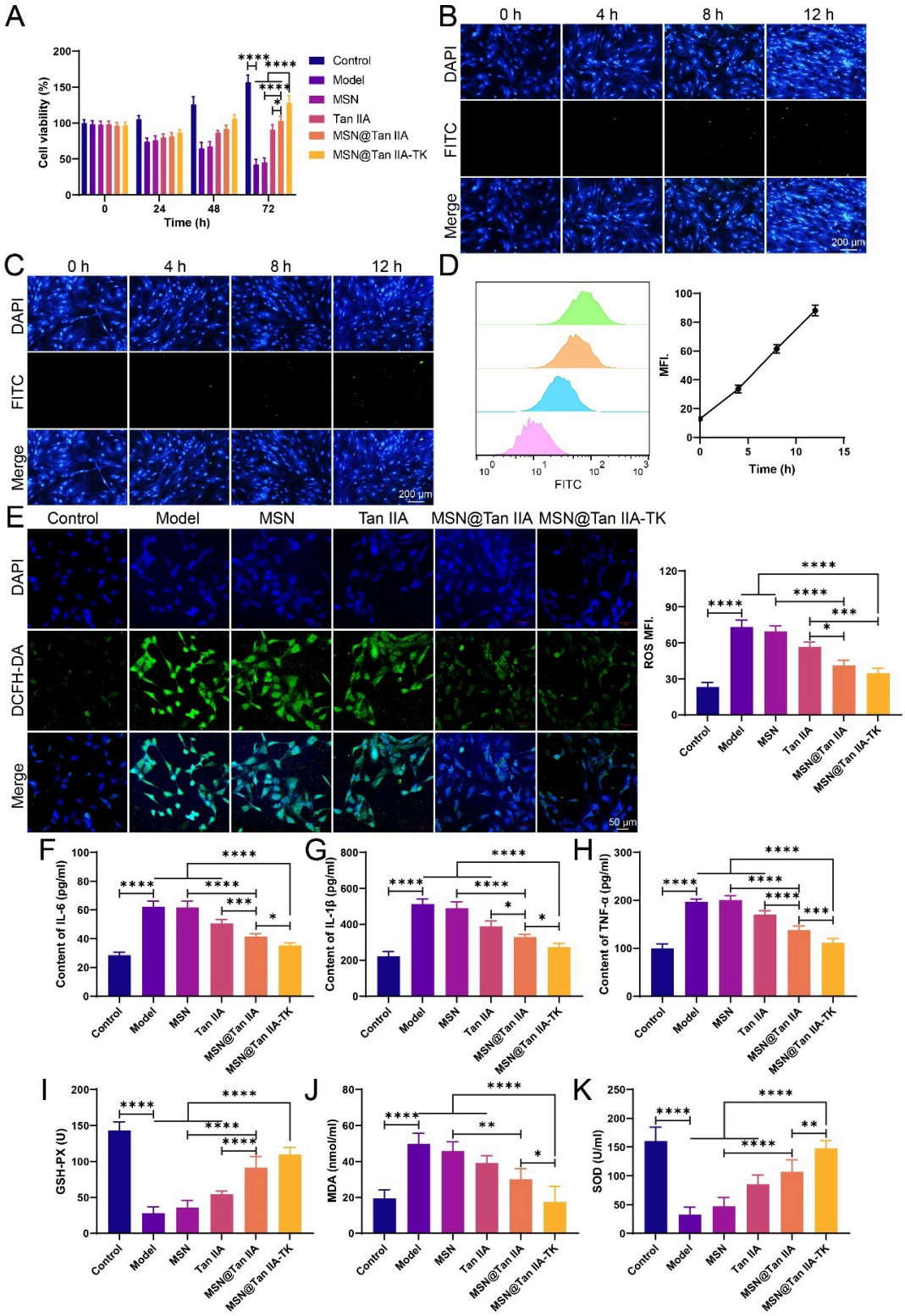


Figure 3

ROS scavenging and inflammation inhibition by MSN@Tan IIA-TK on PCOS cells. (A) Cellular activity of PCOS cells at different times (0h, 24h, 48h, 72h) after different treatments; endocytosis of MSN (B) and MSN@Tan IIA-TK (C) by PCOS cells; (D) quantitative analysis of endocytosis of PCOS cells at different time intervals (0h, 4h, 8h, 12h) on MSN@Tan IIA -TK quantitative analysis of endocytosis; (E) ROS levels in PCOS cells after different treatments using the ROS probe DCFH-DA; (F-K) Changes in inflammatory

factor (IL-6, IL-1β, TNF-α) levels and GSH, MDA, and SOD activities in PCOS cells after different treatments.

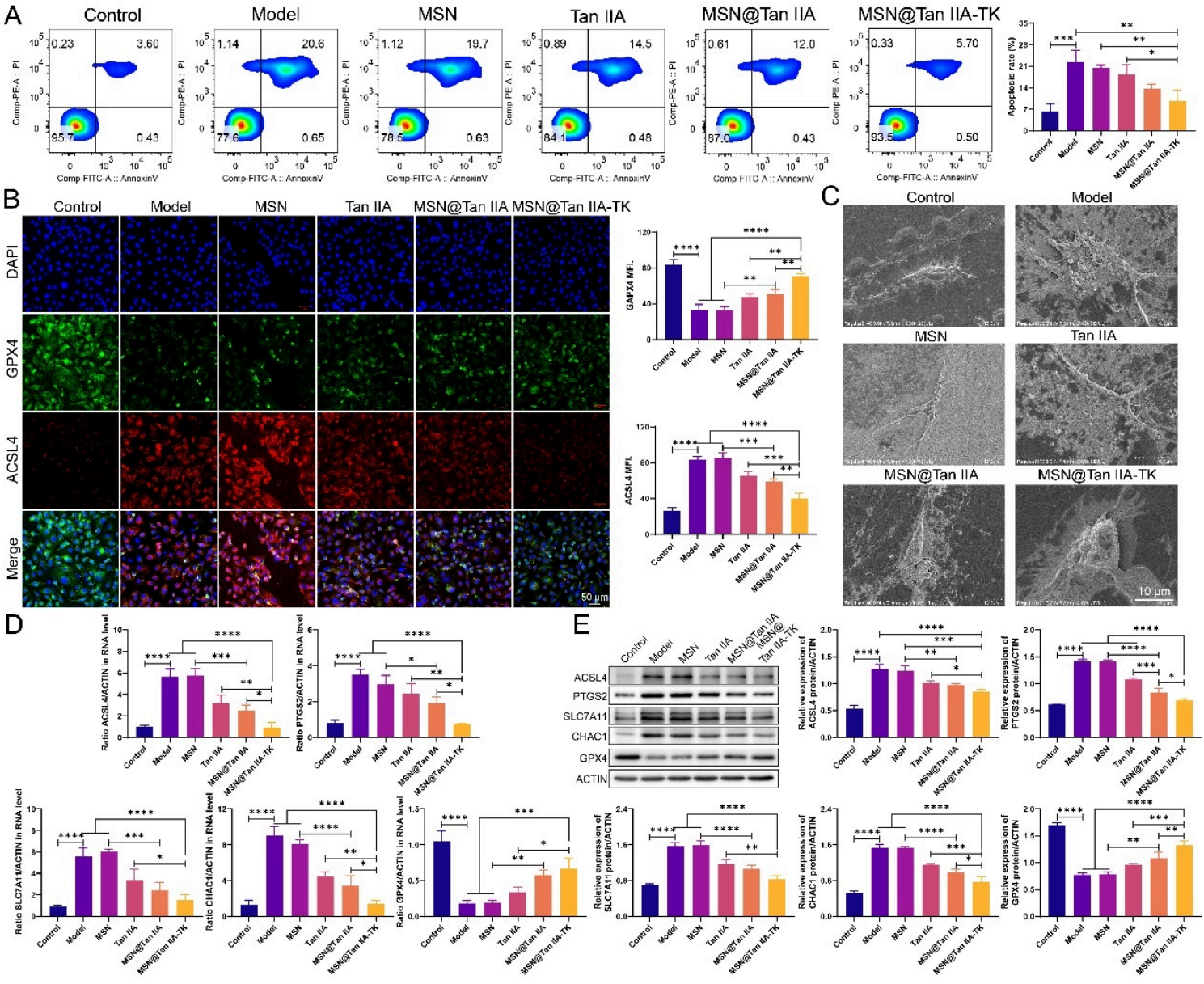


Figure 4

MSN@ Tan IIA-TK effectively inhibited PCOS-induced cell death. (A) Flow cytometry was used to detect the apoptosis level of PCOS cell; (B) immunofluorescence was used to detect the expression level of PCOS cell ferroptosis-related proteins GPX4 and ACSL4; (C) SEM was used to detect the pyroptosis level of PCOS cell; (D) qPCR was used to detect the mRNA expression level of PCOS cell ferroptosis-related genes ACSL4, PTGS2, SLC7A11, CHAC1, and GPX4; (E) Western blot was used to detect the mRNA expression level of PCOS cell ferroptosis-related genes ACSL4, PTGS2, SLC7A11 CHAC1 and GPX4; (E) Western blot was used to detect the protein expression levels of PCOS cell ferroptosis-related genes ACSL4, PTGS2, SLC7A11, CHAC1 and GPX4.

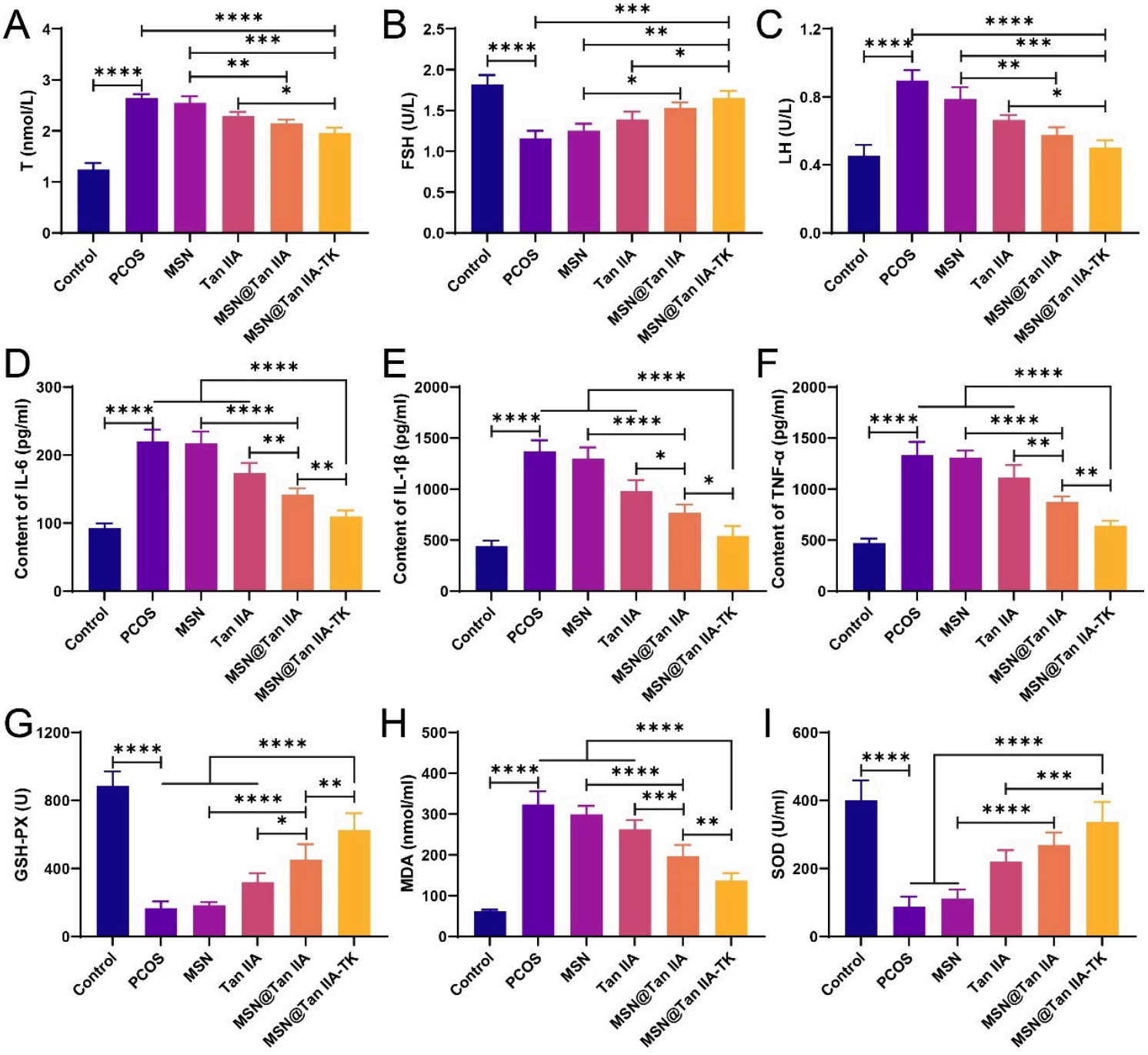


Figure 5

Evaluation of therapeutic effects in PCOS rat model. (A-C) Serum testosterone (T), follicle-stimulating hormone (FSH), and luteinizing hormone (LH) levels in rats; (D-F) Serum inflammatory factors IL-6, IL-1β, and TNF-α levels in rats; (G-I) Changes in serum MDA content and activities of GSH and SOD in rats.

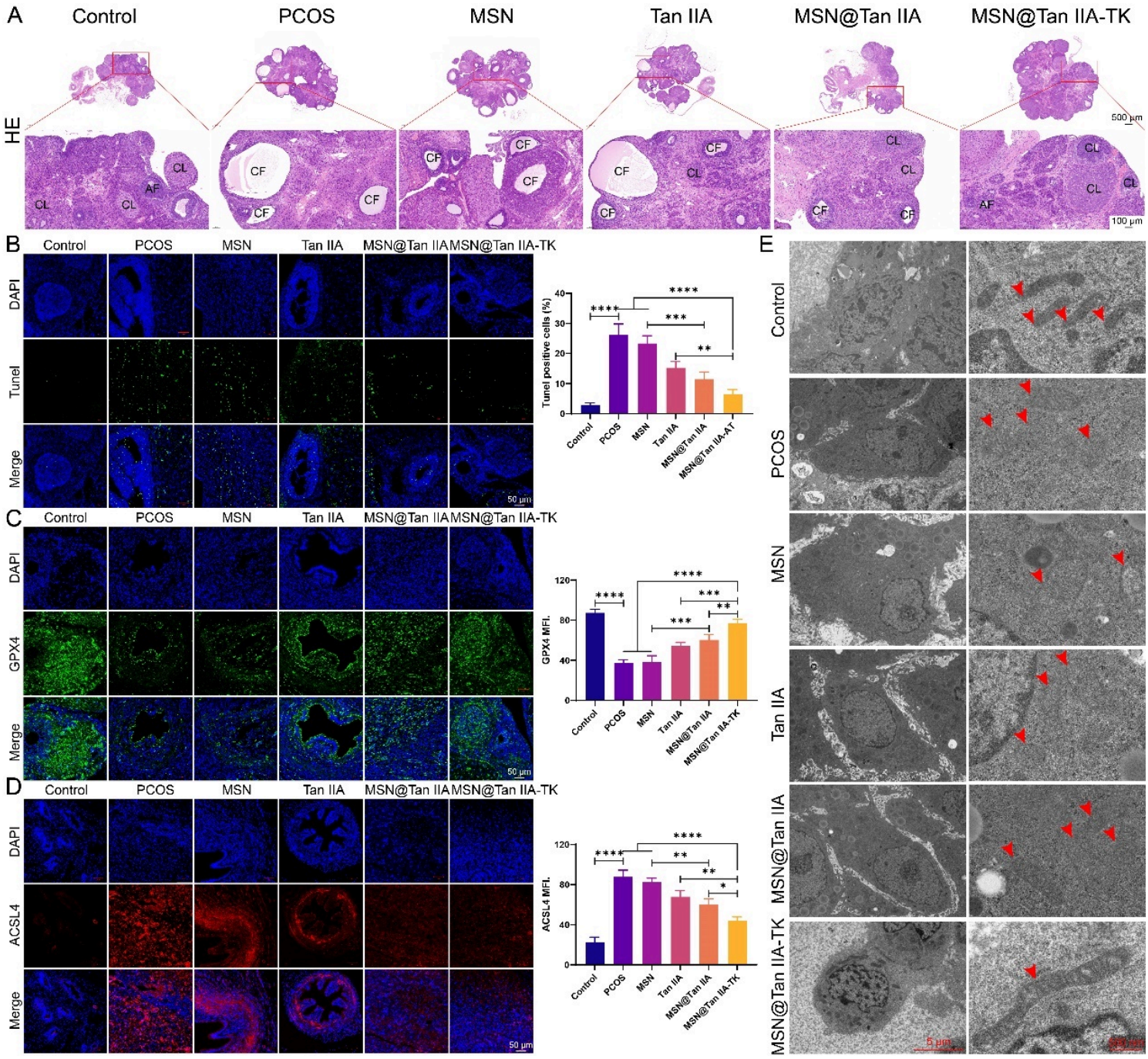


Figure 6

Therapeutic Effects in PCOS Rat Model. (A) Representative images of rat ovarian tissue stained with HE; (B) Representative images of rat ovarian tissue stained with TUNEL; (C-D) Immunofluorescence staining of ferroptosis-related proteins GPX4 and ACSL4 in rat ovarian tissue; (E) TEM image showing mitochondrial morphology in rat ovarian tissue.

Supplementary Files

This is a list of supplementary files associated with this preprint. Click to download.

- SupportingInformation.docx
- floatimage1.jpeg